

## Adsorption and growth of Xe adlayers on the Cu(111) surface

Ji-Yong Park, S.-J. Kahng, U. D. Ham, and Y. Kuk\*

*Department of Physics and Center for Science in Nanometer Scale, Seoul National University, Seoul 151-742, Korea*

K. Miyake and K. Hata

*Institute of Applied Physics and CREST, Japan Science and Technology Corporation (JST), University of Tsukuba, Tsukuba 305-8573, Japan*

H. Shigekawa

*Institute of Applied Physics and CREST, Japan Science and Technology Corporation (JST), University of Tsukuba, Tsukuba 305-8573, Japan*

*and Department of Chemistry and Biotechnology, Graduate School of Engineering, The University of Tokyo, Hongo, Tokyo 113-8656, Japan*

(Received 24 May 1999)

The adsorption and growth of Xe layers on the Cu(111) surface were studied with a low-temperature scanning tunneling microscope. Initially, Xe atoms preferentially adsorb at the step, revealing two different wetting behaviors at the upper and the lower step edges at the coverage of  $<0.1$  monolayer. Three-dimensional island growth is followed on the terrace at the coverage of  $>0.2$  monolayer when grown at  $<20$  K. The island growth is attributed to inhomogeneous nucleation and lower diffusivity of Xe on the Xe monolayer than on the Cu(111) surface. The diffusion barriers, the two-dimensional barrier on a terrace and the one-dimensional barrier along a step, and the step-down barrier determine the growth morphology of Xe layers as the substrate temperature was raised. [S0163-1829(99)00248-9]

### I. INTRODUCTION

Rare-gas layers on various surfaces have been regarded as two-dimensional (2D) model systems due to their closed-shell electronic structure and weak interaction with substrates and among themselves. Because of their simple electronic structures, the adsorbed structures and their transformations with coverage and temperature have been successfully described only with the consideration of simple mutual interaction such as van der Waals interaction. In many experiments, graphite has often been chosen as a substrate due to its weak interaction with rare-gas atoms. Rather complex adsorbed structures were observed when rare gases adsorbed on metal surfaces such as Pt, Ag, Au, Cu, Pd, and Ru.<sup>1</sup> 2D phase transitions such as the commensurate-incommensurate transition (C-I transition), the roughening transition, and the wetting transition are just a few examples of topics which have been studied on various substrates.<sup>1</sup> The wetting behavior has been one of the most studied subjects, as it can be explained as a growth kinetics.<sup>2</sup> When an adsorbate wets the surface and grows in a layer-by-layer mode, the growth behavior is called “complete wetting” [or Frank–van der Merwe (FM) growth]. When an adsorbate grows in a layer-by-layer for initial several layers before three-dimensional (3D) islands are formed on top of them, it is called “incomplete or partial wetting” [or Stranski-Krastanov (SK) growth]. When 3D islands are formed on top of the substrate, it is called “nonwetting” [or Volmer-Weber (VM) growth]. It was shown that the competition between the adatom-substrate interaction and the adatom-adatom interaction determines the growth behavior of rare-gas atoms.<sup>3</sup>

Although many experimental tools have been used to ex-

plore these systems and succeeded in understanding the physics of the rare-gas adsorption, the real-space information is needed for better understanding. Eigler *et al.*<sup>4</sup> first showed isolated Xe atoms adsorbed on Ni(110) and explained the mechanism of how Xe atoms can be imaged with scanning tunneling microscopy (STM) without the apparent electronic states near the Fermi level. The following studies of rare-gas adsorptions have mainly dealt with the subject of atomic manipulation by the STM tip.<sup>5</sup> The adsorption and growth of Xe atoms on Pt(111) were studied by two groups, showing heterogeneous nucleation at defects, followed by layer-by-layer growth.<sup>6,7</sup>

In this paper, the adsorption and growth mode of Xe atoms were studied as functions of coverage and temperature. Xe atoms initially nucleate at the lower step edges and form one-dimensional (1D) chains, and then wet both the lower and upper step edges. With increasing coverage, the Xe layer grows into 3D island structure at the temperature range of 10–20 K.

### II. EXPERIMENT

The experiment was performed with a low-temperature STM with a base pressure of  $<1 \times 10^{-10}$  torr. The whole STM unit can be cooled down to 6 K. A Cu(111) single-crystal sample was cleaned by repeated cycles of Ar<sup>+</sup> ion sputtering and annealing up to 900 K. High-purity Xe gas was dynamically dosed through a stainless-steel tube with a diameter of  $\frac{1}{16}$  in., which is opened at  $\sim 1$  cm away from the cold sample surface by a precision leak valve. This dynamic supply ensured high partial pressure of Xe only around the sample surface, but not in the whole chamber. Although the absolute Xe exposure could not be determined with other surface-science tools, the coverage could be determined with

the dose rate of Xe, the arrival rate multiplied by the exposure time, and STM images. The sample can be annealed by controlling the liquid-helium supply or using a heater attached on the back of the sample. All STM images in this paper were obtained after dosing Xe gas to the Cu surface at 10–20 K.

### III. RESULTS AND DISCUSSIONS

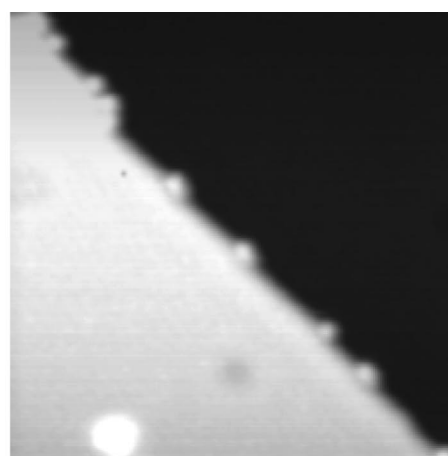
#### A. Growth at low coverage ( $<0.3$ ML)

##### 1. One-dimensional growth at lower step edge

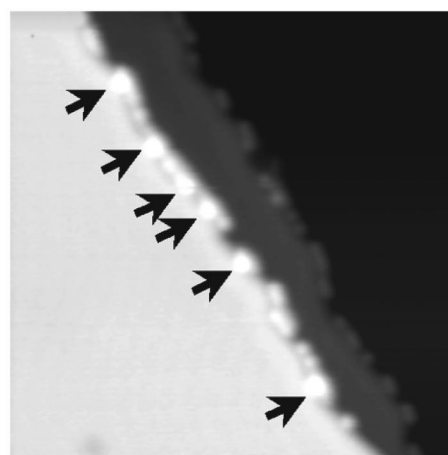
Two different adsorption behaviors were observed with STM when Xe atoms of  $<0.1$  monolayer (ML) were introduced to the metal surface. On a close-packed surface such as Pt(111), they first decorated step edges even at 4 K.<sup>6</sup> On an open surface such as Ni(110), isolated Xe atoms nucleate on the terrace at the low temperature.<sup>4</sup> Figure 1 shows the initial adsorption behavior of Xe atoms on the Cu(111) surface at 10 K. At this low coverage, most of the Xe atoms appear along the step edges, except the ones nucleated at isolated defects or impurities on the terrace. As previously observed in the case of Xe on Pt(111),<sup>6</sup> Xe atoms seem to have large enough transient mobility on the Cu(111) to reach the step edges. However, unlike on the Pt(111) surface,<sup>7</sup> the lower step edges are the first adsorption sites. Figures 1(a) and 1(b) show the first adsorption at the step edges at a coverage of  $\ll 0.1$  ML. In these images, the center of the adsorbed Xe atoms is located at  $1.5 \pm 0.3$  Å away from the Cu lower step edges. Even with a simple atomic superposition calculation,<sup>8</sup> it is easy to conclude that the Xe atoms are located at the lower step edges. There are several missing Xe atoms in the nearly 1D Xe chains. The height of the missing parts is the same as the lower terrace, which is more evidence of the adsorption at the lower step edges. As marked by arrows in Fig. 1(b), some Xe atoms started to occupy the upper step edges with increasing coverage. Figure 1(c) is a perspective view of Fig. 1(b). The arrows in Fig. 1(c) indicate the same Xe atoms that are indicated by arrows in Fig. 1(b). From these images, it can be concluded that most of the Xe atoms adsorb at the lower step edges initially. By further increasing the coverage, the growth of the Xe 1D chain is completed at the lower step edges, but an additional chain is not grown until the first atomic row of Xe is completed. The growth mode of Xe atoms at the lower step edges of Cu(111) can be typified as a ‘‘row-by-row’’ growth. A similar growth mode was observed up to two rows at the step edges on Pt(997) with low-energy helium scattering.<sup>9</sup>

##### 2. Wetting of surface steps

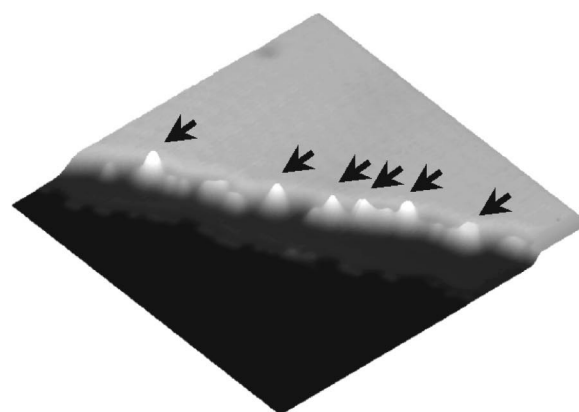
As shown in the preceding section, Xe atoms start to occupy the upper step edges after the growth of one Xe atomic row is almost completed. With increasing coverage ( $>0.08$  ML), the upper step edges are wet as shown in Fig. 2. These changes of the adsorption sites with coverage can be explained with the change of potential well at the lower and upper step edges for Xe atoms. At a very low coverage of Xe, they only decorate the lower step edge, meaning the potential well at the upper step edge is shallower than the thermal energy and the step-edge barrier [Ehrlich-Schwobel (ES) barrier<sup>10</sup>]. Arriving Xe atoms have enough energy to



(a)



(b)



(c)

FIG. 1. STM image of the low-coverage adsorption stage for Xe on the Cu(111) surface. Xe was dosed and imaged at 10 K. (a) All Xe atoms adsorb at the lower step edge ( $200 \times 200$  Å<sup>2</sup>,  $V_s = 0.4$  V,  $I_t = 0.2$  nA). (b) Almost all Xe atoms appear along Cu steps. There are some Xe atoms adsorbed at the upper step edges as marked by arrows ( $300 \times 300$  Å<sup>2</sup>,  $V_s = 0.4$  V,  $I_t = 0.2$  nA). (c) Perspective view of (b). Arrows indicate the same Xe atoms as in (b) which adsorb at upper step edges. Z scale is exaggerated for easier comparison.

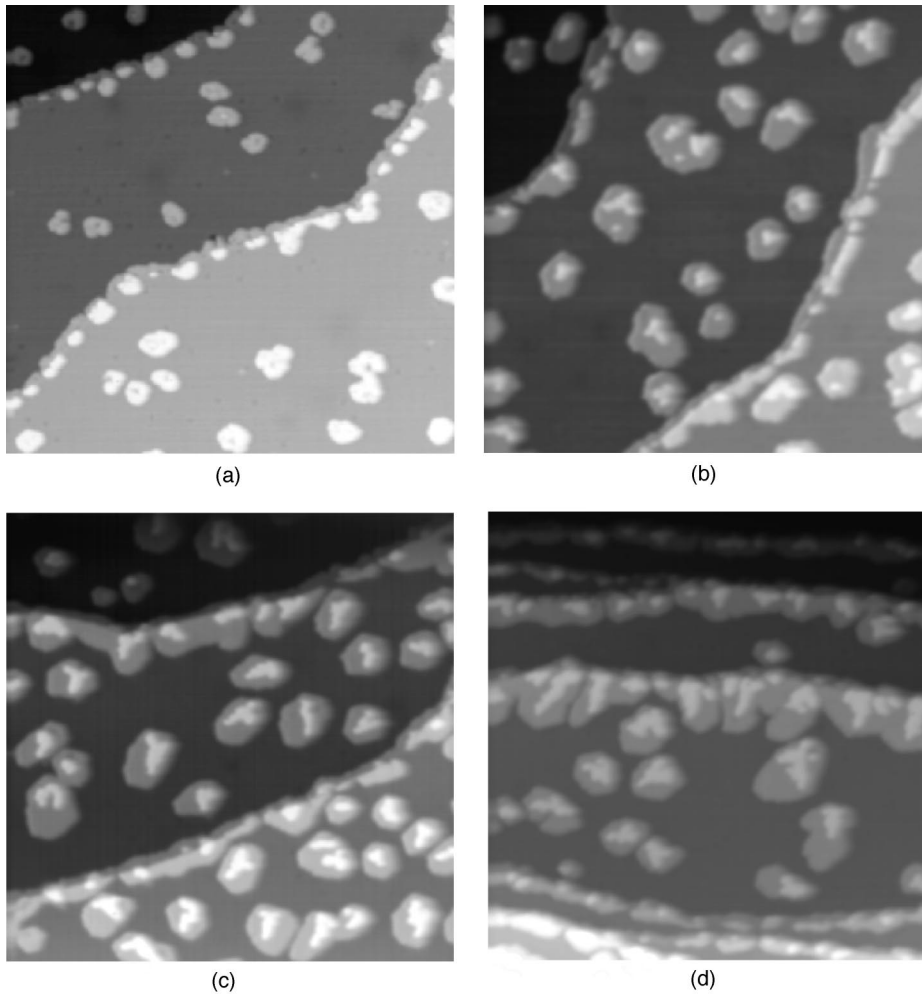


FIG. 2. Images showing wetting of Cu steps by Xe atoms at coverages of (a) 0.08 ML, (b) 0.2 ML, (c) 0.3 ML, and (d) 0.35 ML ( $800 \times 800 \text{ \AA}^2$ ,  $V_s = 0.4 \text{ V}$ ,  $I_t = 0.2 \text{ nA}$ , and  $10 \text{ K}$ ). Note that the morphology at the lower step edges is in sharp contrast with the upper ones. The morphology at the upper step edges changes with increasing coverage, while it remains the same at the lower step edge.

overcome the ES barrier and are trapped at the potential well at the lower step edges. Once they wet the lower step edges with one atomic row, arriving Xe atoms start to occupy upper step edges and form multiple atomic lines as shown in Figs. 1(b) and 2. In the presence of adsorbed Xe atoms at the lower step edges, the potential well at the upper step edge is modified and can accommodate Xe atoms. That may be explained with a modification of the electron density at the step edges with the adsorption of Xe atoms at the lower step edge. Further confirmation may be needed with theoretical calculation.<sup>11</sup>

In Fig. 2, original Cu steps are easily discernible with different growth morphology of Xe atoms between at lower step edges and upper step edges. These growth morphologies can be explained with the 1D wetting behavior with a step acting as a 1D substrate. As can be seen in Fig. 2(a), Xe atoms fully wet the lower step edges to form a thin stripe phase, while Xe atoms “nonwet” the upper step edges to form clusters dispersed along the steps at the low coverage. From Fig. 2, we can see that the wetting characteristics at the upper and lower step edges are quite different from that of the Xe/Pt(111) system, where Xe atoms first adsorb at the upper step edges as a 1D chain, then at the lower step edges.<sup>7</sup> As shown in Fig. 2, the width of the Xe stripe phase at the lower Cu step edges ranges  $10\text{--}20 \text{ \AA}$  ( $3\text{--}6$  monorows) and remains almost the same even at the higher coverage of  $0.1\text{--}0.4 \text{ ML}$ . Unlike at the lower step edge, Xe atoms show mutually attractive interaction at the upper step edges, resulting

in the cluster formation. By further increasing the coverage, Xe layers can form a stripe phase even at the upper step edges similar to the ones at the lower step edges, but much thicker with nonwetting behavior [see Figs. 2(b)–2(d)]. This striking difference between wetting behaviors of Xe between the upper and lower step edges is in sharp contrast to the Xe/Pt(111) case. In one theoretical consideration, Bertel<sup>12</sup> suggested that the Xe atoms at the upper step edge are strongly repulsive in the presence of the Shockley surface state since attractive interaction among Xe atoms through the surface state is absent. As demonstrated in a previous work,<sup>13</sup> a dipole-dipole repulsion created by Xe adsorption is effective in preventing rare-gas atoms from clustering on metal surfaces. Since both Pt(111) and Cu(111) have a surface state with a nearly  $s$  electron nature [ $m^* = 1.3m_e$ ,  $E_B(\bar{\Gamma}) = 400 \text{ meV}$  for Pt(111),<sup>14</sup>  $m^* = 0.46m_e$ ,  $E_B(\bar{\Gamma}) = 390 \text{ meV}$  for Cu(111),<sup>15</sup> respectively,  $m^*$  is the effective mass in the free-electron-like dispersion curve,  $m_e$  the electron mass, and  $E_B(\bar{\Gamma})$  the surface state energy at the  $\bar{\Gamma}$  point of the surface Brillouin zone], observed contrast between two systems seems unusual. At the same time, the lower step edge is usually the preferred adsorption site due to its high coordination number. In view of the similar surface-state properties of these two systems, we speculate that the dipole-dipole interaction around step edges may vary in these two systems.<sup>16</sup> The coverage-independent width of the thin stripe phase at the lower step edges and different wetting behaviors

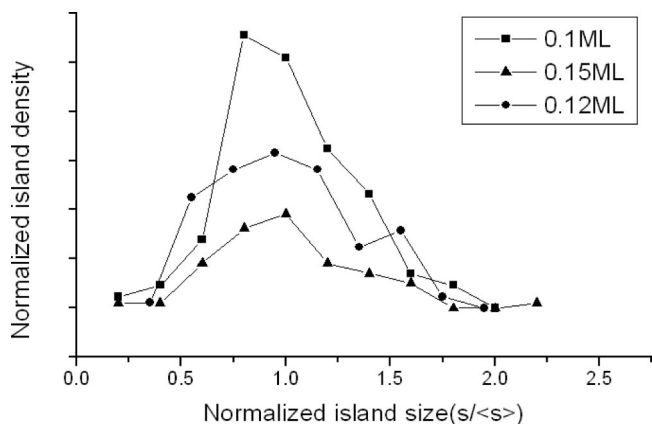


FIG. 3. Normalized density of Xe islands as a function of their relative sizes for three different coverages.

are believed to be the result of the balance between dipole-dipole repulsion and attraction due to its high coordination environment.

## B. Growth at higher coverage

### 1. Nucleation on the terrace

As the coverage exceeds 0.2 ML, Xe islands begin to nucleate on the terraces. Growth behavior can be scaled to a

universal curve since Xe atoms have large diffusivity and are weakly bound to the substrate. In this type of system, the island density of size  $s$ ,  $N_s$ , is scaled as

$$N_s = \frac{\Theta}{\langle s \rangle^2} g\left(\frac{s}{\langle s \rangle}\right), \quad (1)$$

where  $\Theta$  denotes coverage,  $\langle s \rangle$  the average island size, and  $g$  the universal scaling function, respectively.<sup>17,18</sup> The scaling function is plotted at three different coverages in Fig. 3. These three curves, however, do not exactly follow a universal curve as shown in Fig. 3. This slight deviation cannot be explained by strong interactions with the substrate or intermixing between Xe and the substrate. This deviation is mainly due to the fact that Xe atoms nucleate on the Cu terrace only around defects: inhomogeneous nucleation. If there exist defects with large concentration (larger than the density of islands that would otherwise nucleate homogeneously),  $N_s$  is solely determined by the concentration of defects, therefore the deviation from a universal scaling is expected.<sup>17</sup> It was also reported in the Xe/Pt(111) system that Xe islands nucleate around defects or impurities on the terrace.<sup>4,7</sup> It can be concluded that the inhomogeneous nucleation accounts for the clustering of Xe islands on the terrace.

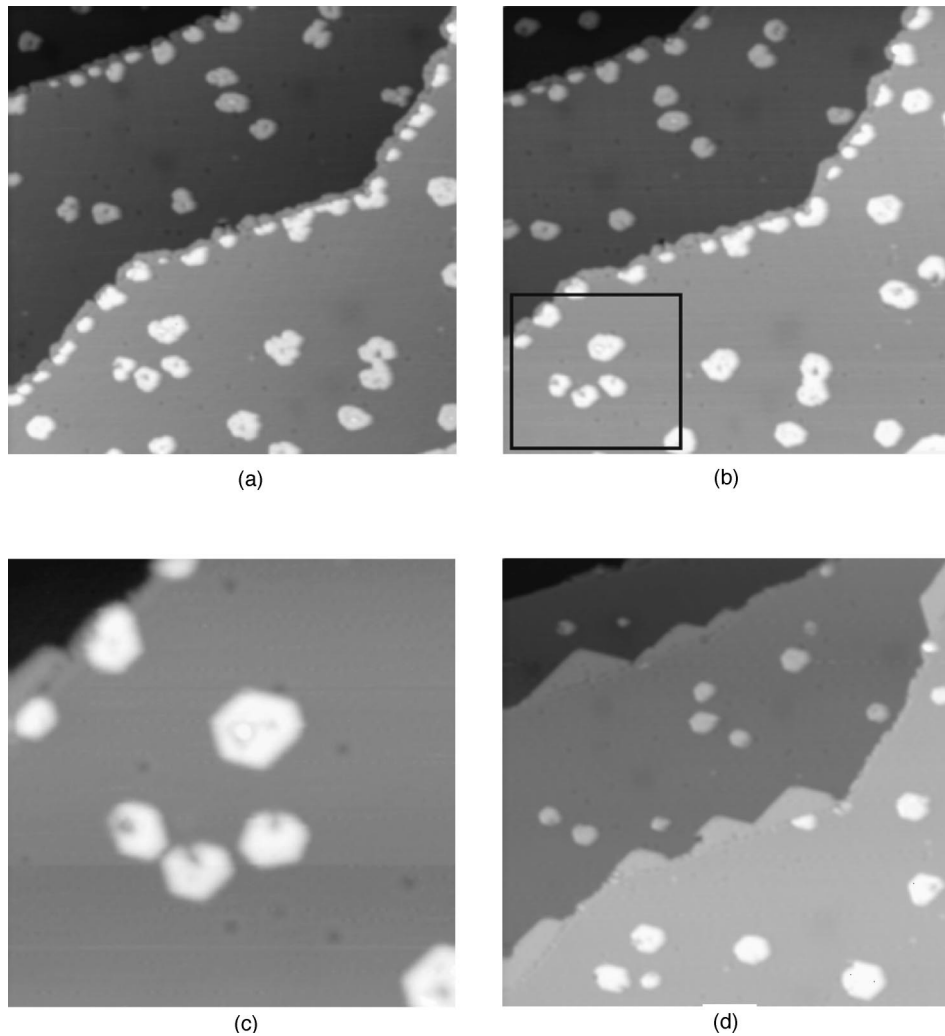


FIG. 4. STM images of morphological changes of Xe as the temperature rises from 10 to 21 K at the same place. For details, see text. (a) 10 K, (b) 15 K, (c) 17 K, zoomed image of the region enclosed by a square in (b), and (d) 21 K [ $800 \times 800 \text{ \AA}^2$  except  $200 \times 200 \text{ \AA}^2$  for (c),  $V_s = 0.4 \text{ V}$ ,  $I_t = 0.2 \text{ nA}$ ].

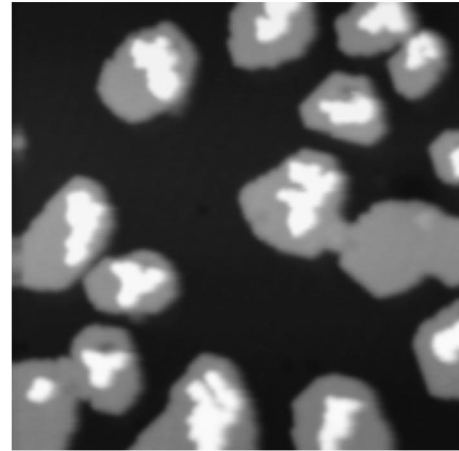
## 2. Temperature-dependent evolution of morphology

Neither noticeable island coarsening nor cluster diffusion was observed in the time scale of several hours at 10 K. We followed the morphological changes at the same location as raising the temperature of the substrate. Comparing the images taken at the same place at the different temperatures below 15 K as in Figs. 4(a) and 4(b), only very small changes due to the diffusion of Xe atoms along the edges of the islands were observed. But as the temperature was raised  $>15$  K, but  $<20$  K, the shape of the Xe islands began to take on a hexagonal shape as shown in Fig. 4(c). Figure 4(c) is an enlarged image of the lower left region of Fig. 4(b) at 17 K. The edges of the Xe islands became sharp at this temperature and the islands began to show hexagonal shapes. As Cu(111) and Xe(111) surfaces have threefold symmetries, the angle between two adjacent  $\{211\}$  planes should be  $120^\circ$  at equilibrium below the roughening transition temperature. In equilibrium, it may show an equilateral hexagon, but many of these are pinned by defects on the Cu substrate, showing a quasiequilibrium, threefold symmetry. Neither noticeable mass transport such as island coarsening nor cluster diffusion was observed at this temperature, suggesting that this equilibrium shape is the result of the diffusion of Xe atoms along the island perimeters. At a temperature of  $>20$  K as in Fig. 4(d), the sharp edges of the hexagonal islands are smoothed, suggesting the roughening transition. All Xe clusters originally adsorbed at the upper step edge diffuse (or move over the ES barrier) to the lower step edges and island coarsening was also observed. The images at higher temperature are not shown here, but at  $>25$  K, Xe atoms began to diffuse from Xe terrace islands to the lower step edges. From these observations, we are able to estimate the order of various barrier heights that Xe atoms experience on the Cu(111) surface. From the temperature dependence, it can be suggested that the barrier for evaporation ( $\Delta E_{ev}$ ) from the island is higher than the step-edge barrier (ES barrier,  $\Delta E_{ES}$ ) and the edge diffusion barrier ( $\Delta E_{ED}$ ):  $\Delta E_{ev} > \Delta E_{ES} > \Delta E_{ED}$ . This order of barrier height is in agreement with the recent result of a calculation for homogeneous diffusion of Al on the Al(111) surface.<sup>19</sup>

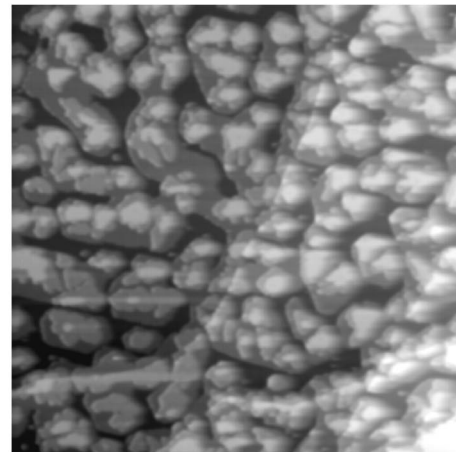
## 3. Multilayer growth

By further increasing Xe coverage, 3D island growth was observed at a temperature range of 10–20 K. The second- and third-layer Xe islands are shown in Figs. 5(a) and 5(b). The STM tip often drags Xe atoms at the third layer, resulting in frequent tip changes or degradation of the STM images. As Xe atoms physisorb on the surface, the atoms can be easily pulled or pushed depending on the polarity of the STM tip. It has been reported that the STM tip could be used to manipulate weakly bound Xe atoms on metal surfaces.<sup>5</sup> In order to make sure that our scanning process did not disturb the morphology, we checked the images by scanning with various bias voltages and tunneling currents at the same place. The tunneling conditions without any changes on the morphology before and after the scan were chosen.

From observation of this multilayer growth, Xe atoms seem to “nonwet” the Cu(111) surface at 10 K. As stated in the Introduction, it has been shown that the growth behavior of rare gas on a substrate can be scaled according to the interaction strength.<sup>2</sup> The growth behavior can be explained



(a)



(b)

FIG. 5. STM images of 3D island growth. (a) Second-layer Xe islands ( $800 \times 800 \text{ \AA}^2$ ,  $V_s = 0.4 \text{ V}$ ,  $I_t = 0.2 \text{ nA}$ , and 10 K). (b) Third-layer Xe islands ( $2000 \times 2000 \text{ \AA}^2$ ,  $V_s = 0.4 \text{ V}$ ,  $I_t = 0.2 \text{ nA}$ , and 16 K).

by the ratio  $u/h$  (where  $u$  is the adatom-substrate interaction with which isosteric heat of adsorption is taken and  $h$  is the adatom-adatom interaction with which 0 K cohesive energy of the bulk phase is taken).<sup>2</sup> Complete wetting (FM growth) takes place only when the ratio  $u/h$  is around 1. The incomplete wetting (SK growth) occurs when the ratio is less than or more than 1. Nonwetting (VM growth) is observed when the ratio is much less than 1.<sup>2</sup> Although there are some exceptions to this theory,<sup>20</sup> many known systems follow this trend. In the case of Xe on the Cu(111) surface, layer-by-layer growth of the Xe multilayer on the Cu(111) surface was observed at  $>20$  K (Ref. 21) [15 K, in the case of polycrystalline Cu (Ref. 22)]. Despite the nonwetting of Xe on the Cu(111) surface at 10 K as observed here, our results agree well with the earlier results of complete wetting behavior at higher temperature with an enhanced interlayer mass transport at  $>20$  K as shown in Fig. 4(d). It can be suggested that there should be a phase transition from nonwetting to incomplete or complete wetting at a temperature range of 15–25 K, based on our observation.

## 4. Difference in diffusivity

As described in Sec. III B 1, the first-layer Xe islands nucleate around the defects on the Cu surface. These defects

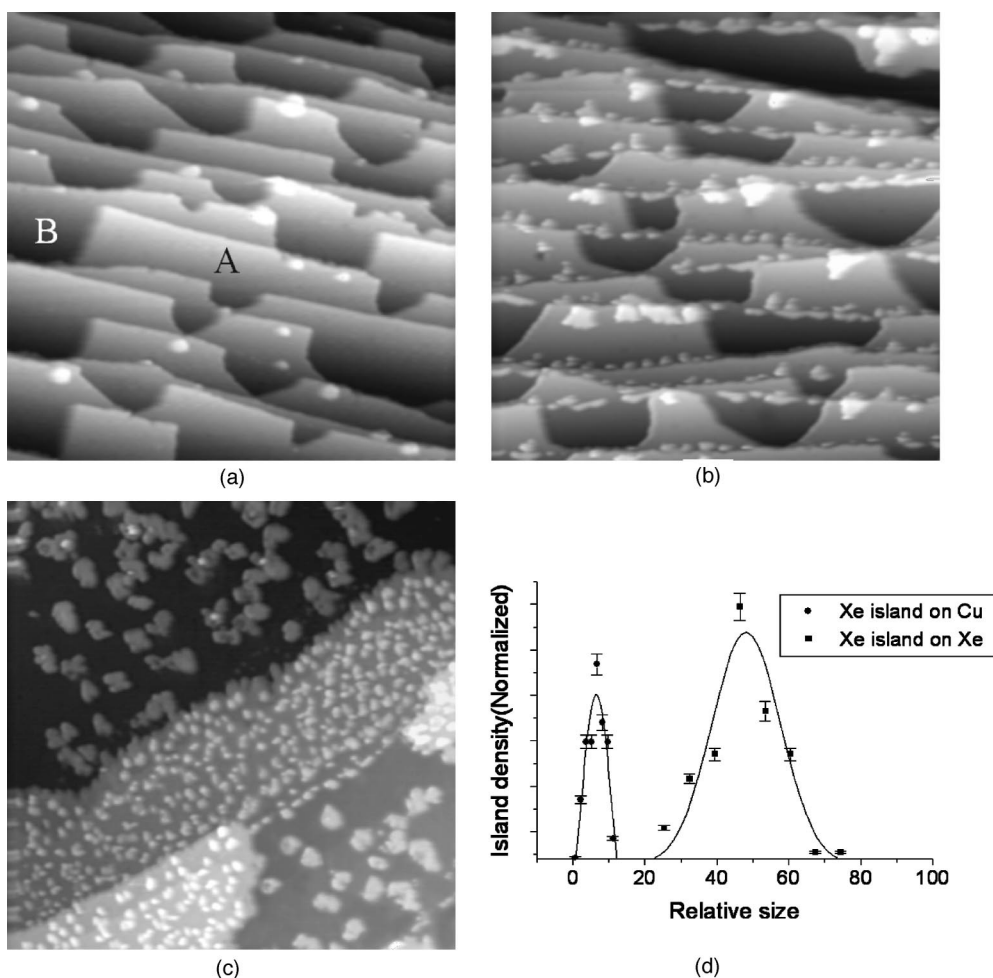


FIG. 6. (a) One-monolayer-high Xe patches cover the half of the surface. The image was taken after Xe was first dosed at 10 K, annealed to  $>30$  K, and quenched to 10 K again. *A* denotes the Xe monolayer patch and *B* denotes the clean Cu surface, for example. (b) Xe of  $\sim 0.05$  ML was additionally dosed on the surface similar to (a) at 10 K ( $800 \times 800 \text{ \AA}^2$ ,  $V_s = 0.4$  V,  $I_t = 0.2$  nA). (c) Prepared in the same way as (b), but about 0.7 ML on the larger terrace ( $1600 \times 1600 \text{ \AA}^2$ ,  $V_s = 0.4$  V,  $I_t = 0.2$  nA, and 14 K). (d) Island density distribution as a function of island size for both the “Xe on Xe” and “Xe on Cu” cases. Solid lines are Gaussian fits for each datum.

can accommodate potential wells for Xe atoms to nucleate not only on the Cu surface but also on the Xe layer. However, this inhomogeneous nucleation mechanism alone cannot explain the observed different shapes of multilayer islands. As seen in Fig. 5, the shapes of second-layer Xe islands are quite different from those of the first-layer Xe islands; the first-layer islands are those of nearly equilibrium, but the second-layer islands are those of diffusion-limited aggregation. Usually the layer-by-layer growth mode is determined by the competition between in-plane diffusivity and the ES barrier.<sup>23</sup> In the present observation, the second-layer islands nucleate at the center of the first layer and grow to irregularly shaped islands. This can be explained by the fact that diffusivity is the determining factor in 3D island growth. The large difference in diffusivity between “Xe on Cu” and “Xe on Xe” was observed at a temperature range of 10–20 K. To elucidate this effect further, about 0.5 ML of Xe was dosed at 10 K, resulting in 3D island growth, and the sample was annealed to  $>30$  K. After it was cooled down to 10 K, additional Xe was introduced on the surface again to grow Xe islands on the bare Cu substrate and the large Xe first layer at the same time. Figure 6(a) shows a typical image just after cooling. As expected, about half of the surface is cov-

ered with a Xe monolayer while the other half exposes the bare Cu surface. White spots are additional Xe clusters, strongly pinned at defects during the annealing procedure. As an additional  $\sim 0.05$  ML of Xe gas was introduced to the surface at 10 K, the image became quite different from the one just after the cooling. Because this imaged region has a higher step density than other regions imaged previously, only a few Xe islands are visible here. The region around the boundary between bare Cu terraces and Xe terraces shows substantial differences. The Xe atoms spread along the boundary on the Cu terrace to form a stripe phase. However, isolated Xe cluster structures grow from the lower step edges, indicating reduced diffusivity along the lower edges of the Xe layer. When we have large terraces, we can compare the difference of diffusivity by measuring island density as in the case of Fig. 6(c). The sizes of the Xe islands on the Xe terraces are much smaller and the densities are higher than those on the Cu terraces, meaning lower diffusivity of Xe atoms on top of Xe terraces than on the Cu substrate. According to a model which relates the density and size of the islands to diffusivity,<sup>24</sup> the island density  $N$  is proportional to  $D^{-1/3}$ , where  $D$  is the diffusion coefficient. From the observed island distribution on each layer as in Fig. 6(d),

we were able to estimate that  $D_{\text{Xe}_{\text{Cu}}}$ , the diffusion coefficient of “Xe on Cu,” is about 350 times larger than  $D_{\text{Xe}_{\text{Xe}}}$ , the diffusion coefficient of “Xe on Xe.” This large difference in diffusivity prevents Xe atoms that adsorb on top of the existing first-layer Xe islands from diffusing to the edge and stepping down to the Cu terrace, resulting in the observed 3D island growth. As the binding energy of Xe on first-layer Xe is smaller than on the Cu substrate, this small diffusivity is unusual. The observed diffusivity difference may be explained with two possible mechanisms. First, the binding energy among Xe atoms is much lower on the Xe monolayer than on the Cu substrate, explaining the small Xe island size on top of the first layer. Second, the difference may be explained with transient mobility. As we showed earlier in this paper about the low-coverage growth, Xe atoms show high transient mobility on Cu(111) at around 10 K. We think that the low diffusivity on the Xe monolayer can result from the fact that the transient mobility of the Xe atoms is more easily dissipated on the Xe layer than on the Cu surface.

#### IV. CONCLUSION

We have presented growth modes and mechanisms of Xe atoms adsorbed on the Cu(111) surface with low-temperature STM. We have identified the first adsorption site as the lower

step edge at low temperature, in contrast to the Pt(111) surface. It was shown that the upper step edge could be an attractive site for Xe atoms, possibly due to the reduced dipole-dipole repulsion resulting from the redistribution of electrons. We found that the density of Xe islands does not follow the scaling behavior due to the inhomogeneous nucleation. The relative order of barrier heights was determined (the barrier for evaporation from island edges  $>$ ES barrier  $>$ edge diffusion barrier) from the temperature-dependent morphology. We found that Xe islands on top of the Cu surface at around 17 K reveal quasi-two-dimensional thermal equilibrium shape. For high coverage growth, 3D island growth was found for Xe atoms on top of the Cu surface around 10 K. This 3D island growth is thought to occur due to much reduced diffusivity for the “Xe on Xe” compared to the “Xe on Cu” case at low temperature and inhomogeneous nucleation.

#### ACKNOWLEDGMENTS

This work was partially supported by Korean Ministry of Science and Technology through the Creative Research Initiative Program. Support from a Grant-in-Aid for Scientific Research from the Ministry of Education, Science, Sport and Culture of Japan is also acknowledged.

\*Author to whom correspondence should be addressed. Electronic address: ykuk@phy.snu.ac.kr

<sup>1</sup>For reviews of these systems, see *Phase Transitions in Surface Films 2*, edited by H. Taub, G. Torzo, H. J. Lauter, and S. C. Fain, Jr. (Plenum, New York, 1991); *Ordering in Two Dimensions*, edited by S. K. Sinha (North-Holland, Amsterdam, 1980).

<sup>2</sup>J. L. Seguin, J. Suzanne, M. Bienfait, J. G. Dash, and J. A. Venables, *Phys. Rev. Lett.* **51**, 122 (1983); M. Bienfait, J. L. Seguin, J. Suzanne, E. Lerner, J. Krim, and J. G. Dash, *Phys. Rev. B* **29**, 983 (1984).

<sup>3</sup>D. E. Sullivan, *Phys. Rev. B* **20**, 3991 (1979).

<sup>4</sup>D. M. Eigler, P. S. Weiss, E. K. Schweizer, and N. D. Lang, *Phys. Rev. Lett.* **66**, 1189 (1991).

<sup>5</sup>D. M. Eigler and E. K. Schweizer, *Nature (London)* **344**, 524 (1990); D. M. Eigler, C. P. Lutz, and W. E. Rudge, *ibid.* **352**, 600 (1991); Björn Neu, Gerhard Meyer, and Karl-Heinz Rieder, *Mod. Phys. Lett. B* **9**, 963 (1995).

<sup>6</sup>P. S. Weiss and D. M. Eigler, *Phys. Rev. Lett.* **69**, 2240 (1992).

<sup>7</sup>P. Zeppenfeld, S. Horch, and G. Comsa, *Phys. Rev. Lett.* **73**, 1259 (1994); Sebastian Horch, Peter Zeppenfeld, and George Comsa, *Surf. Sci.* **331-333**, 909 (1995).

<sup>8</sup>J. Tersoff and D. R. Hamann, *Phys. Rev. Lett.* **50**, 1998 (1983); *Phys. Rev. B* **31**, 805 (1985).

<sup>9</sup>V. Marsico, M. Blanc, K. Kuhnke, and K. Kern, *Phys. Rev. Lett.* **78**, 94 (1997); V. Pouthier, C. Ramseyer, C. Girardet, K. Kuhnke, V. Marsico, M. Blanc, R. Schuster, and K. Kern, *Phys.*

*Rev. B* **56**, 4211 (1997).

<sup>10</sup>G. Ehrlich and F. G. Hudda, *J. Chem. Phys.* **44**, 1039 (1966); R. L. Schwoebel, *J. Appl. Phys.* **37**, 3682 (1966).

<sup>11</sup>N. D. Lang and J. Yu (private communication).

<sup>12</sup>E. Bertel, *Surf. Sci.* **367**, L61 (1996).

<sup>13</sup>A. Jablonski, S. Eder, K. Markert, and K. Wandelt, *J. Vac. Sci. Technol. A* **4**, 1510 (1986).

<sup>14</sup>P. Roos, E. Bertel, and K. D. Rendulic, *Chem. Phys. Lett.* **232**, 537 (1995).

<sup>15</sup>S. D. Kevan, *Phys. Rev. Lett.* **50**, 526 (1983).

<sup>16</sup>M. D. Thompson and H. B. Huntington, *Surf. Sci.* **116**, 522 (1982).

<sup>17</sup>M. C. Bartelt and J. W. Evans, *Phys. Rev. B* **46**, 12 675 (1992).

<sup>18</sup>A.-L. Barabási and H. E. Stanley, *Fractal Concepts in Surface Growth* (Cambridge University Press, Cambridge, 1995).

<sup>19</sup>A. Bogicevic, J. Strömquist, and B. I. Lundqvist, *Phys. Rev. Lett.* **81**, 637 (1998).

<sup>20</sup>K. Kern, R. David, R. L. Palmer, and G. Comsa, *Phys. Rev. Lett.* **56**, 2823 (1986).

<sup>21</sup>J. Jupille, J. J. Ehrhardt, D. Fargues, and A. Cassuto, *Vacuum* **41**, 399 (1990).

<sup>22</sup>J. E. Demuth, Ph. Avouris, and S. Schmeisser, *Phys. Rev. Lett.* **50**, 600 (1983).

<sup>23</sup>N. Memmel and E. Bertel, *Phys. Rev. Lett.* **75**, 485 (1995).

<sup>24</sup>Y. W. Mo, J. Kleiner, M. B. Webb, and M. G. Lagally, *Phys. Rev. Lett.* **66**, 1998 (1991).